Journal of proteome research

Article

pubs.acs.org/jpr

Profiling Carbonylated Proteins in Heart and Skeletal Muscle Mitochondria from Trained and Untrained Mice

Andrea Carpentieri,[‡,¤] Tania Gamberi,[†,¤] Alessandra Modesti,[†] Angela Amoresano,[‡] Barbara Colombini,[§] Marta Nocella,[§] Maria Angela Bagni,[§] Tania Fiaschi,[†] Lorenzo Barolo,[‡] Massimo Gulisano,[§] and Francesca Magherini*[,†]

[†]Department of Experimental and Clinical Biomedical Sciences "Mario Serio", University of Florence, Viale G.B. Morgagni 50, Florence, 50134 Italy

[‡]Department of Chemical Sciences, Federico II University, Complesso Universitario Monte Sant'Angelo, Via Cinthia 4, 80126 Naples, Italy

[§]Department of Experimental and Clinical Medicine, University of Florence, Viale G.B. Morgagni 63, 50134 Florence, Italy

Supporting Information

ABSTRACT: Understanding the relationship between physical exercise, reactive oxygen species, and skeletal muscle modification is important in order to better identify the benefits or the damages that appropriate or inappropriate exercise can induce. Heart and skeletal muscles have a high density of mitochondria with robust energetic demands, and mitochondria plasticity has an important role in both the cardiovascular system and skeletal muscle responses. The aim of this study was to investigate the influence of regular physical activity on the oxidation profiles of mitochondrial proteins from heart and tibialis anterior muscles. To this end, we used the mouse as animal model. Mice were divided into two groups: untrained and regularly trained. The carbonylated protein pattern was studied by two-dimensional gel electrophoresis followed by Western blot with anti-dinitrophenyl hydrazone antibodies. Mass spectrometry analysis allowed the identification of several different protein oxidation sites, including methionine, cysteine, proline, and leucine residues. A large number of oxidized proteins were found in both untrained and trained animals. Moreover, mitochondria from skeletal muscles and heart showed almost the same carbonylation pattern. Interestingly, exercise training seems to increase the carbonylation level mainly of mitochondrial proteins from skeletal muscle.

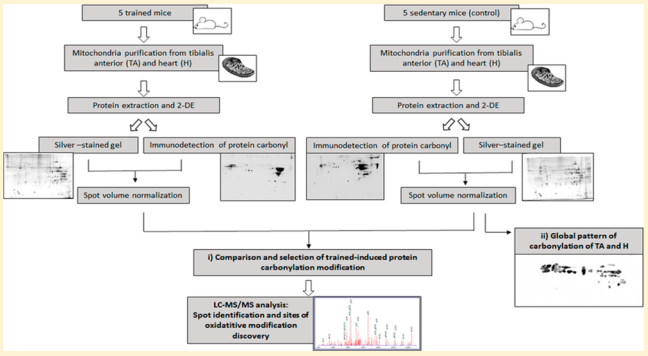

KEYWORDS: *training, exercise, mice, redox proteomics, oxyblot, two-dimensional gel electrophoresis (2-DE), tandem mass spectrometry (MS/MS), protein oxidation, protein carbonylation, reactive oxygen species (ROS)*

INTRODUCTION

A proper practice of regular physical exercise has many health benefits, including cardiovascular protection, reduction of the risk of obesity and of diabetes, reinforcement of joints, hormonal control, and aging delay. How physical exercise affects muscles depends on both mode, intensity, and duration of training and specific characteristics of the skeletal muscle in question. In skeletal muscles, reactive oxygen (ROS) and nitrogen species (RNS) are normally synthesized at low levels. They are also required for normal force production and are necessary for oxidative stress-related adaptation.[1] On the other hand, intense physical activity and its relative increase in oxygen consumption can lead to an imbalance between production and disposal of ROS, and this can induce the establishing of a condition of "oxidative stress".

Several potential sources of ROS, likely to be activated by different stimuli, have been identified in muscle cells. Among these are mitochondria, nicotinamide adenine dinucleotide phosphate (NADPH) oxidases (NOXs), phospholipase A2 (PLA2), xanthine oxidase (XO), and lipoxygenases.[2] Recently, Sakellariou et al.[3] demonstrated that NADPH oxidase is the major source of acute cytosolic ROS increase at rest and during contractile activity. Nevertheless, the same group described an increase of superoxide in mitochondria that is stimulated by contractions but occurs over a slower and delayed time course.[4] This suggests that acute and longer term contraction protocols may activate different sources of superoxide generation and could explain the contradictions present in the literature on this topic. Inside the mitochondria complex I and complex III[5−7] are important sites of superoxide production. New findings also identify complex II (succinate dehydrogenase) as a major source of superoxide production, and it was shown that the contribution of each site to total H_2O_2 production is strongly

Received: May 25, 2016
Published: August 29, 2016

DOI: 10.1021/acs.jproteome.6b00475
J. Proteome Res. 2016, 15, 3666−3678

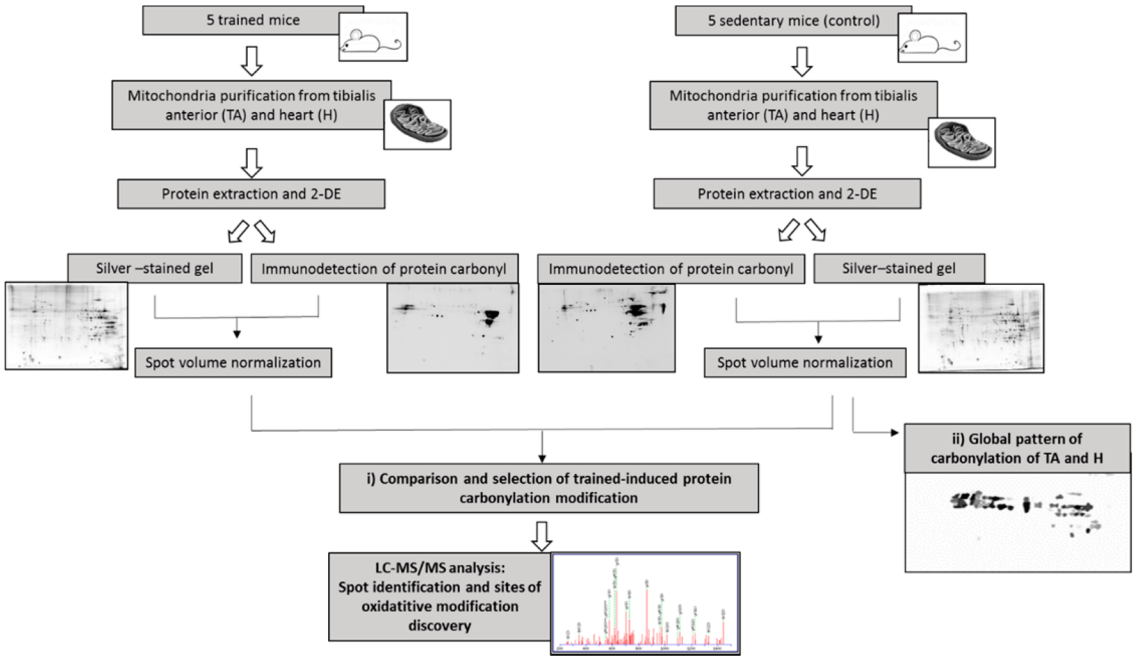

Figure 1. Experimental workflow overview.

dependent on the substrate being oxidized.[8,9] Currently, the estimation of oxygen fraction, released from the mitochondria as superoxide, is about 0.15% of the total amount of oxygen used,[10] and this estimation is thus lower than the one, 2−5%, calculated previously.[11] Furthermore, it has been demonstrated that mitochondria produce higher ROS during state 4 of respiration (non ADP-stimulated respiration) than in state 3 (basal respiration). This point is very interesting, since, during contraction, mitochondria are prevalent in state 3, i.e. under low ROS production conditions. In this context, the study of the mitochondrial protein oxidation pattern under basal conditions and after regular training could help to better understand the impact of exercise on this organelle.

In particular, we focused our attention on protein carbonylation, an oxidative modification that occurs in several processes. These include physiological processes, such as aging and exercise; and pathological processes, such as Alzheimer's disease, Parkinson's disease, cancer, cataractogenesis, diabetes, and sepsis.[12,13] Carbonyl derivatives can be formed by a direct metal catalyzed oxidation (MCO) of the side chains of proline, arginine, lysine, and threonine residues and by oxidative cleavage of the peptide bond. In addition, carbonyl derivatives can result from an indirect reaction of the primary amino-groups of lysine with reduced sugar or their oxidation product and by a Micheal addiction reaction of lysine, cysteine, and histidine residues with α,β-unsaturated aldehydes formed during peroxidation of polyunsaturated fatty acids. The effect of different types of exercise on plasma and muscle protein carbonylation was deeply investigated in many studies. Most of the studies only report the total amount of carbonyl groups without identifying the proteins that are specific targets of oxidation.[14−20] Despite this, these studies present a complex pattern of carbonylation that seems to be affected by several factors, such as the type of exercise performed, level of training of the subject, and timing of the sample. The identification, by the proteomic approach, of the proteins that undergo a carbonylation level modification following exercise was only described in a few studies.[21−24] These studies concern plasma protein carbonylation and muscle protein carbonylation. No study has been performed selectively on mitochondria that play a key role in both metabolism and ROS production. The discovery of carbonylation of mitochondrial proteins could be greatly improved starting from highly purified mitochondrial subcellular fractions. In fact, the resulting reduction of sample complexity can lead to the identification of proteins that can be muffled from high expressed proteins in a total cellular extract.

Here we describe how carbonylation affects mitochondrial proteins from skeletal muscle and heart, under basal conditions and after regular training in mice. In particular, carbonylated proteins were identified by derivatization of the carbonyl group with 2,4-dinitrophenylhydrazine (DNPH), which leads to the formation of a stable 2,4-dinitrophenyl (DNP) hydrazone product. The DNP adducts were assessed by two-dimensional gel electrophoresis followed by Western blot immunoassay (Oxyblot). Carbonylated proteins, as well as their carbonylation sites, were identified by mass spectrometry (MS).

The goal of this study was to identify proteins in mice mitochondria from skeletal muscle and heart that were oxidized *in vivo* and, in particular, to answer the following questions: (i) Does carbonylation affect to the same extent mitochondria isolated from different tissues (i.e., skeletal muscle and heart)? (ii) Is the carbonylation pattern modified by regular exercise? (iii) Which are the main sites of carbonylation? A complete overview of the workflow was shown in Figure 1.

EXPERIMENTAL SECTION

Animal Models and Endurance Training

This study was carried out in compliance with the guidelines of the European Communities Council Directive 2010/63/UE and the recommendations for the care and use of laboratory animals approved by the animal care Committee of the University of Florence (Italy). Mice (C57BL/6, male, aged three months at entry) were housed in a controlled temperature room (21−24 °C) with a 12−12 h light−dark cycle. Food and water were provided *ad libitum*. All mice were

DOI: 10.1021/acs.jproteome.6b00475
J. Proteome Res. 2016, 15, 3666−3678

familiarized with a horizontally rotating treadmill (Hai-PanLab 5 lanes Treadmill) for 10 min on 2 consecutive days. During this acclimatization period, each mouse sat in the treadmill chamber resting or running (speed was gradually increased from 5 to 25 cm/s). After each familiarization bout, the mice were returned to their cages with free access to food and water. The third day mice were randomly assigned to either a sedentary or exercised group. The exercise program was based on previous studies[25−27] and consisted of a training frequency of 5 days/week for 8 weeks.

Mice were progressively trained in order to obtain the desired workload intensity (~80% of VO_{2max}) in 2 weeks.[25,27] This workload was maintained for 6 weeks. The training session lasted 45 min: 2 min of familiarization at 0 cm/s, 6 min warm-up at increasing treadmill speed from 5 to 34 cm/s; 15 min of continuous running at 34 cm/s; 5 min recovery at 16 cm/s; 15 min of continuous running at 34 cm/s; 2 min of cool-down with decreasing speed from 34 to 0 cm/s. The treadmill slope was 10° during the whole period of training. The untrained control animals were placed on the switched-off treadmill for the same amount of time as for the training sessions.

All animals were killed by rapid cervical dislocation;[28] exercised mice were sacrificed 24 h after the last training. Heart and tibialis anterior muscle were removed immediately and used for mitochondria purification.

Mitochondria Purification

Mitochondria were purified according to Frezza et al. with minor modifications.[29] Briefly, heart and tibialis anterior were removed from mice immediately after the sacrifice, and immersed in 5 mL of ice-cold PBS supplemented with 10 mM EDTA. Muscles were then minced into small pieces, washed twice in the same buffer, and finally resuspended in 5 mL of ice-cold PBS supplemented with 10 mM EDTA and 0.05% trypsin for 30 min. The minced muscles were then centrifuged at 200*g* for 5 min and the pellet was resuspended in 2 mL of homogenation buffer (obtained by mixing 6.7 mL of 1 M sucrose, 5 mL of 1 M Tris/HCl, 5 mL of 1 M KCl, and 1 mL of 1 M EDTA in a volume of 100 mL in distilled water, pH 7.4). The samples were then homogenized using a Teflon pestle by stroking the minced samples ten times. The homogenate was centrifuged at 700*g* for 10 min at 4 °C, and the supernatant was recovered and centrifuged at 8,000*g* for 10 min at 4 °C. The pellet was resuspended in 8 M urea, 4% (w/v) CHAPS, and 50 mM DTT.

2-DE and Immunodetection of Protein Carbonyls (2-DE Oxyblot)

Protein samples (60 μg for Oxyblot, 20 μg for silver stained gels, and 120 μg for preparative gels) were separated on 11 cm immobilized pH gradient (IPG) strips (pH 3−8 NL) on a PROTEAN i12 IEF System (BIO-RAD). In particular, the strips were actively rehydrated (at 50 V), for 14 h, in the presence of sample in rehydration solution (8 M urea, 2% (w/v) CHAPS, 0.5% (w/v) DTE) supplemented with 0.5% (v/v) carrier ampholyte (Bio-Rad) and a trace of bromophenol blue. The strips were then focused at 16 °C according to the following electrical conditions: 250 V for 20 m (rapid), from 250 to 8000 V for 1 h, 8000 V until a total of 26000 V/h was reached, with a limiting current of 50 μA/strip. After first dimension protein carbonyls were derivatized to DNP (2,4-dinitrophenylhydrazone) by incubating IPG strips in 10 mM DNPH (2,4-dinitrophenylhydrazine, Sigma-Aldrich) dissolved in 2 N HCl, for 20 min at room temperature.

Following derivatization, the marked IPG strips were washed with 6 M urea, 20% (v/v) glycerol, 1% (w/v) SDS, 150 mM Tris-HCl, pH 6.8, and then they were reduced, alkylated, and run on 4−16% precast polyacrylamide gels (BIO-RAD). After running, gels were blotted on a polyvinylidene fluoride (PVDF) membrane. The PVDF membranes were incubated overnight at 4 °C with the primary antibody solution consisting of a 1:10,000 dilution of anti-DNP IgG antibody (Sigma) in phosphate-buffered saline (PBS) containing 2.0% nonfat dry milk. The blots were then washed with PBS, 0.1% (v/v) Tween and incubated with the goat antirabbit IgG/HRP conjugate (1:3,000 dilution in PBS/Milk) for 1 h at room temperature. Gels used for normalization of Oxyblots were stained with ammoniacal silver nitrate as previously described;[30] MS-preparative gels were stained with brilliant blue colloidal Coomassie.[31]

Image Acquisition and Analysis

Gel and Oxyblot images were acquired using an Epson expression 1680 PRO scanner and saved as TIFF files. Computer-aided 2D image analysis was carried out using ImageMaster 2D Platinum software version 6.0 (GE Healthcare). Relative spot volume (%V = V single spot/V total spots, where V is the integration of the optical density over the spot area) was used during analysis in order to reduce experimental error. The volume of carbonylated spots on Oxyblots was normalized vs their respective spots visualized on silver stained gels. The efficiency and the reproducibility of the blotting was always checked by staining the PVDF membrane with brilliant blue Coomassie. Differences in spot carbonylation level between untrained and trained mice were determined using Student's two tailed independent *t* test. P-values of ≤0.05% were considered significant.

Proteins Identification by LC-MS/MS Analysis

Carbonylated spots were *in situ* hydrolyzed with trypsin, and peptide mixtures thus obtained were directly analyzed by LTQ Orbitrap XL hybrid ion trap-orbitrap mass spectrometry (Thermo Fisher Scientific, Bremen, Germany). C-18 reverse phase capillary column 75 μm*10 cm (Thermo Fisher Scientific) chromatography was performed using a flow rate of 300 nL/min, with a gradient from eluent A (0.2% formic acid in 2% acetonitrile) to eluent B (0.2% formic acid in 95% acetonitrile). The following gradient conditions were used: t = 0 min, 5% solvent B; t = 10 min, 5% solvent B; t = 90 min, 50% solvent B; t = 100 min, 80% solvent B; t = 105 min, 100% solvent B; t = 115 min, 100% solvent B; t = 120 min; 5% solvent B. Peptides analysis was performed using data-dependent acquisition of one MS scan followed by CID and ETD fragmentations of the three most abundant ions. For the MS/MS experiment, we selected the three most abundant precursors and subjected them to sequential CID-MS/MS and ETD-MS/MS acquisitions. For the MS scans, the scan range was set to 400−1800 m/z at a resolution of 60,000, and the automatic gain control (AGC) target was set to 1×10^6. For the MS/MS scans, the resolution was set to 15,000, the AGC target was set to 1×10^5, the precursor isolation width was 2 Da, and the maximum injection time was set to 500 ms. The CID normalized collision energy was 35%; the charge-dependent ETD reaction time was enabled, and the ETD AGC target was set to 1×10^5. Data were acquired by Xcalibur software (Thermo Fisher Scientific). Peaklists were generated by Mass Matrix data converter software version 3.9 directly from each raw data.

DOI: 10.1021/acs.jproteome.6b00475
J. Proteome Res. 2016, 15, 3666−3678

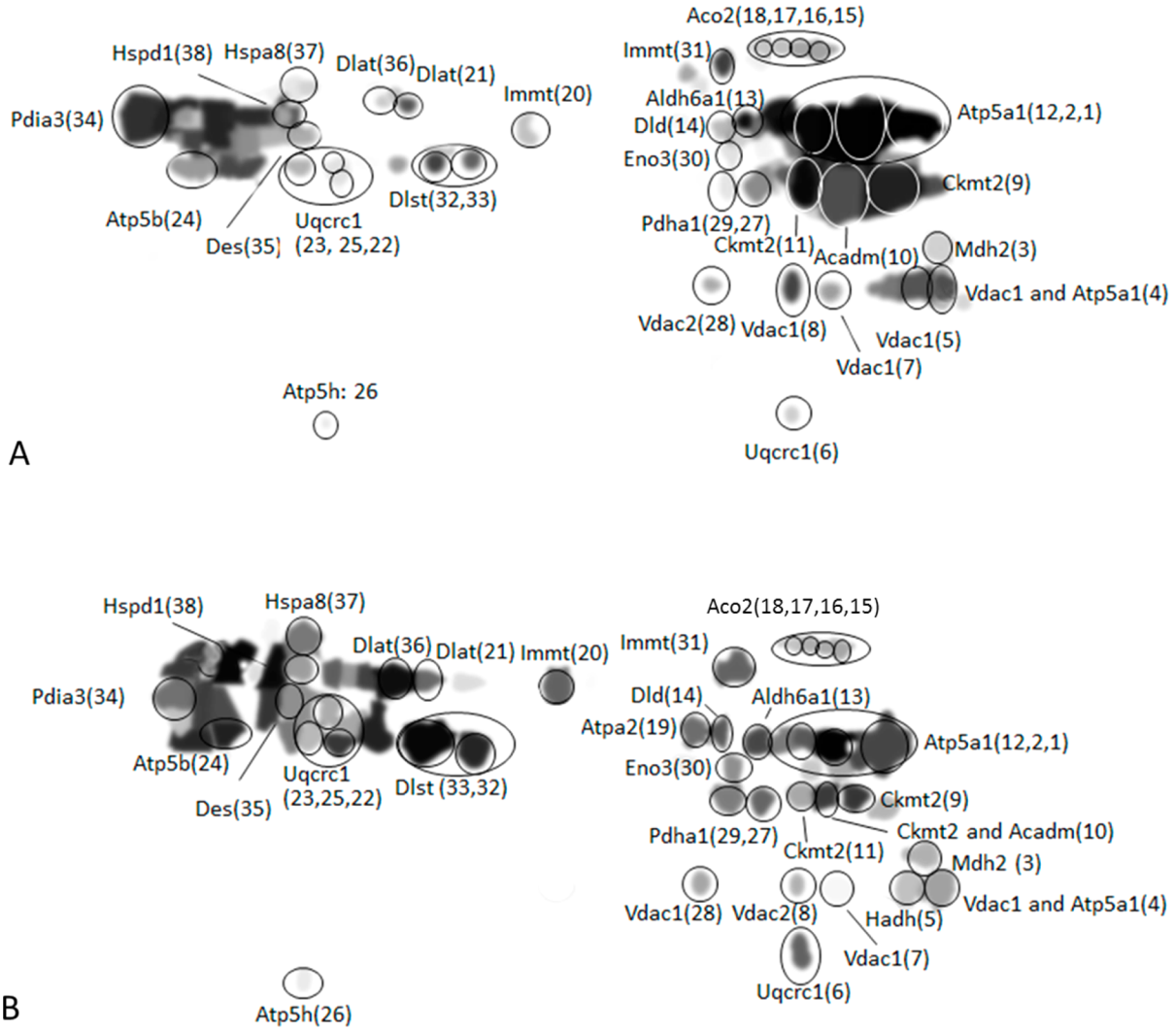

Figure 2. Synthetic Oxyblots representing the carbonylation pattern of H (A) and TA (B) muscles. These images were composed with the Oxyblot images from all untrained mice and show only the carbonylated spots matched in at least four of the five images obtained from muscle samples. The spots identified by MS were indicated.

In-house Mascot software (version 2.4.0) was used as a search engine to identify proteins and their modification sites. The database used for protein identification was SwissProt 2015_02 (547,599 sequences; 195,014,757 residues); we used as search parameters trypsin as protease to generate peptides, maximum 3 missed cleavages allowed, 10 ppm as peptide mass tolerance, 0.6 Da as fragment mass tolerance, carbamidomethyl (C) as fixed modification, and Arg → GluSA (R), cysteic acid (C) (C), deamidated (NQ), Gln → pyro-Glu (N-term Q), His-oxo His (H), hydroxylation (K) (K), hydroxylation (P) (P), Nitro (Y), Leu-HydroxiLeu (L), Lys → Allysine (K), oxidation (HW), oxidation (M), Pro → pyro-Glu (P), Pro-GluSA (P), S-hydroxycysteine (C), Thr-KetoButyricacid (T) as variable modifications.

Bioinformatics and Statistical Analysis

Carbonylated proteins were used as input list in order to obtain a categorization and an over-representation analysis (ORA) using the Webgestalt online tool ("WEB-based GEne SeT AnaLysis Toolkit") (http://www.webgestalt.org/) against Gene Ontology (GO) and WikiPathway.[32] The statistics performed in the over-representation analysis (ORA) dealt with the p-value obtained from the Fisher exact test followed by the p-value adjusted for multiple testing by the Benjamini–Hochberg correction. The input list was furthermore analyzed by R spider.[33] The molecular networks inferred by spider tools are profiled according to three different models, named D1, D2, and D3. In model D1 are considered only the direct interactions between proteins list, while in models D2 and D3 are allowed one and two intermediate nodes, respectively. We analyzed the input list allowing the insertion of one intermediate node (model D2). The p-value provided was computed by the Monte Carlo simulation (http://www.bioprofiling.de/statistical_frameworks.html) and referred to as the probability of obtaining a model of the same quality for a random gene list of the same size.[34] The significant networks, using a cutoff of $p < 0.01$, were further considered for proteomic data interpretation and discussion. The enriched network was exported as a .xgmml file, visualized, and modified by Cytoscape 3.1.0 (http://www.cytoscape.org/).[35]

DOI: 10.1021/acs.jproteome.6b00475
J. Proteome Res. 2016, 15, 3666−3678

Table 1. Identity of H and TA Muscle Spots Resulted Carbonylated in Untrained Mice

AC	Gene name	Protein name	Spot number	Molecular process (GO biological process)
Q03265	Atp5a1	ATP synthase subunit alpha, mitochondrial	1H,2H,4H[a],12H, 1TA,2TA, 4TA[a],12TA	ATP biosynthetic process GO:0006754
P56480	Atp5b	ATP synthase subunit beta, mitochondrial	24H 24TA	ATP biosynthetic process GO:0006754
Q9DCX2	Atp5h	ATP synthase subunit d, mitochondrial	26H 26TA	ATP synthesis coupled proton transport GO:0015986
Q9CZ13	Uqcrc1	Cytochrome *b*-c1 subunit 1, mitochondrial	6H,22H,23H,25H 6TA,22TA,23TA,25TA	Mitochondrial electron transport, ubiquinol to cytochrome c GO:0006122
Q6P8J7	Ckmt2	Creatine kinase S-type, mitochondrial	9H,11H 9TA,10TA[a],11TA	Phosphocreatine metabolic process GO:0006603
Q8CAQ8	Immt1	MICOS complex subunit Mic60	20H, 31H 20TA, 31TA	Cristae formation GO:0042407
Q60932	Vdac1	Voltage-dependent anion-selective channel protein 1	4H[a],5H,7H, 28H 4TA[a],7TA,28TA	Anion transport GO:0006820
Q60930	Vdac2	Voltage-dependent anion-selective channel protein 2	8H 8TA	Anion transport GO:0006820
		Mitochondrial matrix (GO cellular component)		
P45952	Acadm	Medium-chain specific acyl-CoA dehydrogenase, mitochondrial	10H 10TA[a]	Fatty acid beta-oxidation GO:000663
Q61425	Hadh	Hydroxyacyl-coenzyme A dehydrogenase, mitochondrial	5TA	Fatty acid beta-oxidation GO:0006635
P35486	Pdha1	Pyruvate dehydrogenase E1 component subunit alpha, somatic form, mitochondrial complex, mitochondrial	27H,29H 27TA,29TA	Acetyl-CoA biosynthetic process from pyruvate GO:0006086
Q8BMF4	Dlat	Dihydrolipoyllysine-residue acetyltransferase component of pyruvate dehydrogenase complex, mitochondrial	21H, 36H 21TA,36TA	Acetyl-CoA biosynthetic process from pyruvate GO:0006086
O08749	Dld	Dihydrolipoyl dehydrogenase, mitochondrial	14H 14TA	Dihydrolipoyl dehydrogenase activity GO:0004148
Q9D2G2	Dlst	Dihydrolipoyllysine-residue succinyltransferase component of 2-oxoglutarate dehydrogenase	32H,33H 32TA,33TA	Tricarboxylic acid cycle GO:0006099
P08249	Mdh2	Malate dehydrogenase, mitochondrial	3H 3TA,4TA	Tricarboxylic acid cycle GO:0006099
Q99KI0	Aco2	Aconitate hydratase, mitochondrial	15H,16H,17H,18H 15TA,16TA,17TA,18TA	Tricarboxylic acid cycle GO:0006099
Q9EQ20	Aldh6a1	Methylmalonate-semialdehyde dehydrogenase [acylating], mitochondrial	13H 13TA	Valine and tyamine catabolic process GO:0006574 and GO:0006210
P56480	Atp5b	ATP synthase subunit beta, mitochondrial	24H 24TA	ATP biosynthetic process GO:0006754
P63038	Hspd1	60 kDa heat shock protein, mitochondrial	38H 38TA	Response to unfolded protein GO:0006986
P63017	Hspa8	Heat shock cognate 71 kDa protein	37H 37TA	mRNA processing GO:0006397
P31001	Des	Desmin	35H 35TA	Cytoskeletal protein binding GO:0008092
P21550	Eno3	Beta enolase	30H 30TA	Glycolytic process GO:0006096
O55143	Atp2a2	Sarcoplasmic/endoplasmic reticulum calcium ATPase 2	19TA	Calcium ion import into sarcoplasmic reticulum GO:1990036
P27773	Pdia3	Protein disulfide-isomerase A3	34H 34TA	Cell redox homeostasis GO:0045454

[a]Indicates spots in which two different proteins were identified; see also the text. The first column is accession numbers in Swiss-Prot/UniprotKB (www.uniprot.org/).

RESULTS

Global Pattern of Carbonylated Proteins in Skeletal Muscle and Heart of Untrained Mice

In order to verify whether carbonylation affects to the same extent mitochondria from skeletal muscle and heart, mitochondria were isolated by heart (H) and tibialis anterior (TA) muscle from untrained mice. Mitochondrial proteins were separated by 2-DE, and Oxyblot was performed. To evaluate if the basal level of carbonylation was the same in the mitochondria isolated from these two different tissues, the images of all Oxyblots were used to perform two synthetic Oxyblot images (mitochondrial proteins from TA and H) in which only spots present at least in 4 samples (on a total of 5 samples analyzed) were taken into account. This type of image is obtained by averaging the positions, shapes, and optical densities of the spots in a given set of Oxyblot images (representative images of TA and H Oxyblot from control animals were shown in Figure 7). Figure 2 reports the synthetic Oxyblot obtained from TA (A) and H (B) Oxyblots. These synthetic images represent the common carbonylation pattern that can be found in the mitochondria of these two types of muscles. In these images we found 53 and 51 carbonylated spots in TA and H, respectively. In order to identify these spots, preparative gels were performed and colloidal Coomassie stained (Figure 1S). The Oxyblot images and the PVDF stained membranes were matched to the images of preparative gels in order to excide the selected spots for mass spectrometry analysis. The increment of protein load caused an expected loss of separative power, and some carbonylated spots were not clearly detected or resolved in Coomassie stained gels. Due to this imprecise overlapping between these two types of images, 11 and 10 carbonylated spots in TA and H, respectively (especially in the acid region of the gels), could not be localized with certainty and were left out. Therefore, 42 spots from TA and 41 spots from H were in situ hydrolyzed with trypsin, and the resulting peptide mixtures were extracted from the gel and submitted to nanoLC/MS/MS analysis by using a high-resolution LTQ Orbitrap XL mass spectrometer, generating sequence information on individual peptides. This information, together with the peptide mass values, was then used to search protein databases, leading to the identification of the protein components. Each protein mixture was run through LC/MS/MS three times, and the identified protein spots (38 from TA and 37 from H) are summarized in Table 1 (detailed MS data were reported in Table 1S). In some cases, more than one

DOI: 10.1021/acs.jproteome.6b00475
J. Proteome Res. 2016, 15, 3666−3678

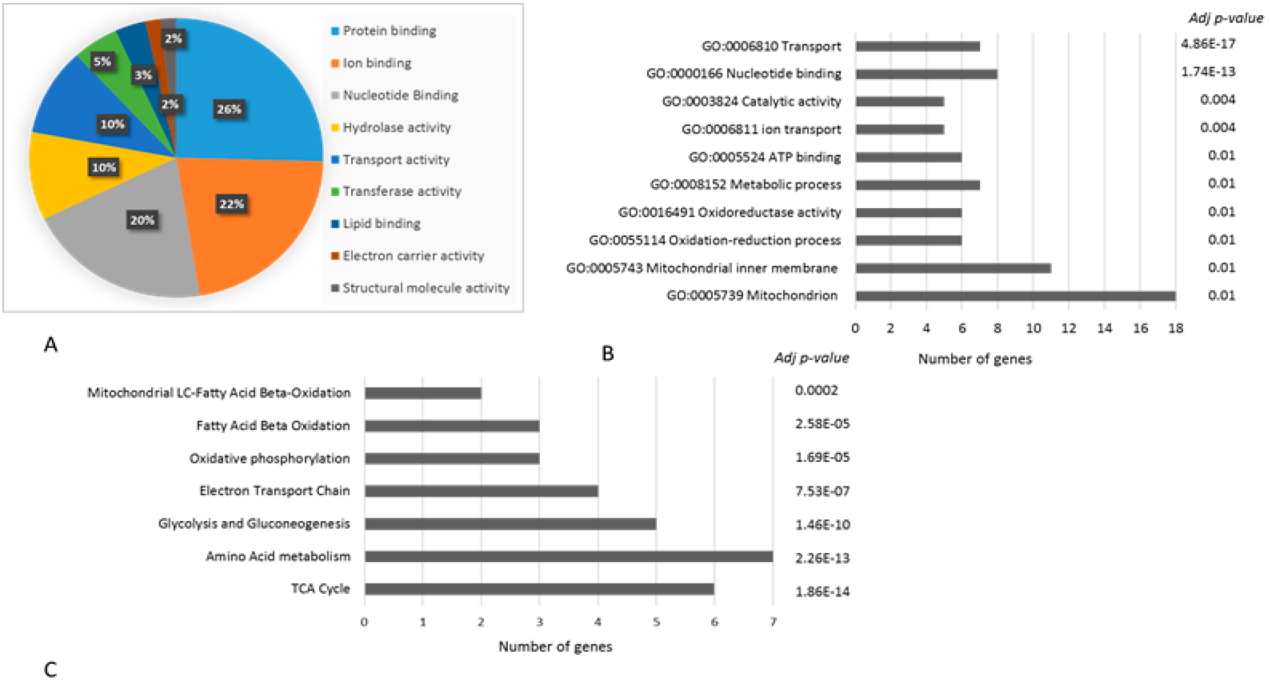

Figure 3. (A) Pie chart representation of identified protein distributions according to their molecular functions. Categorizations were based on information provided using the online resource WebGestalt (http://www.webgestalt.org/) classification system. In (B) and (C) the enriched GO terms (ProfCom_GO) and pathways (Wikipathways) were reported.

protein was detected in a single spot (these spots are indicated with the letter "a" in Table 1). Furthermore, some proteins were detected in more than one spot; these spots are usually characterized by having a different isoelectric point, probably due to different post-translation modifications, including oxidative ones (e.g., Vdac1, Atp5a1, Ckt2). The identified proteins are located in the mitochondrial membrane (19 spots in TA and 19 spots in H) and in the matrix (22 spots in TA and 20 in H). The list of the identified proteins includes mitochondrial proteins and a few nonmitochondrial proteins, indicating the specificity of the purification method utilized to achieve the enriched mitochondrial fraction. Two of these proteins (protein disulfide-isomerase A3 and sarcoplasmic/endoplasmic reticulum calcium ATPase 2) belong to the endoplasmic reticulum (ER), whose components can be purified with mitochondria since mitochondria and ER are closely associated and are structurally and functionally related.[36] The identification of desmin can be explained considering that this protein is a scaffolding protein with a role of anchoring mitochondria to the cytoskeleton, and so, it could likely be copurified with mitochondria.[37]

Identified proteins were grouped into nine sets (Figure 3A), according to their molecular functions. The enriched gene ontology (GO) terms and pathways are also reported in Figure 3B and Figure 3C, respectively. As shown, proteins involved in the TCA cycle, amino acid metabolism, electron transport chain, and oxidative phosphorylation are highly represented. Concerning OXOPHOS complexes, spots found as carbonylated correspond to proteins of complex V (7 spots) and complex III (4 spots in H and 4 in TA); carbonylation of proteins belonging to the other complexes was not detected. In the matrix we identified proteins of the pyruvate dehydrogenase complex (2 spots), of the Krebs cycle (7 spots), and of the beta oxidation pathway (2 spots) (see Table 1 for GO Biological process classification).

To gain a deeper insight into the pattern of carbonylated proteins and to establish whether these proteins have common interactors, the list of carbonylated spots was enriched in terms of a network-based statistical framework. A pathway-based network was built by allowing the insertion of one intermediate node using the Reactome database in the Bioprofiling platform (www.bioprofiling.de). By allowing the insertion of one intermediate node (model D2), an interconnected network was obtained (Figure 4). In this network, 10 nodes (rectangles) overlapped with the input list and intermediate nodes (triangles) were the enriched ones. In deep gray and light gray, the most representative pathways, corresponding to the TCA cycle and valine, leucine, and isoleucine degradation pathways, are indicated. Dihydrolipoamide S-acetyltransferase (E2 component of pyruvate dehydrogenase complex, DLAT), dihydrolipoamide S-succinyltransferase (E2 component of 2-oxo-glutarate complex, DLST), and dihydrolipoamide dehydrogenase (DLD) have in common a lipoamide molecule as cofactor (DLST and DLAT) or as substrate (DLD). The enzyme citrate synthase resulted in an intermediate node connected with five proteins of the input list. With the exception of aconitase, all these proteins are dehydrogenases (MDH2, PDH1, DLD) or belong to a protein complex with dehydrogenase activity (DLAT) and have a nucleotide binding domain. Also, the proteins found in leucine and isoleucine degradation pathways (ACADM, HLDH, HADH) are dehydrogenases and have a nucleotide binding domain.

It is noteworthy that carbonylation was not directly dependent on protein concentration, so that there were intense spots in the Coomassie stained PVDF membrane and in silver-stained gels that did not display a perceptible carbonylation or present a very low carbonylation level (spots 22 and 25, corresponding to cytochrome *b*-c1 complex subunit 1, mitochondrial); meanwhile, other protein spots present at low concentration in silver-stained gels exhibited important

DOI: 10.1021/acs.jproteome.6b00475
J. Proteome Res. 2016, 15, 3666−3678

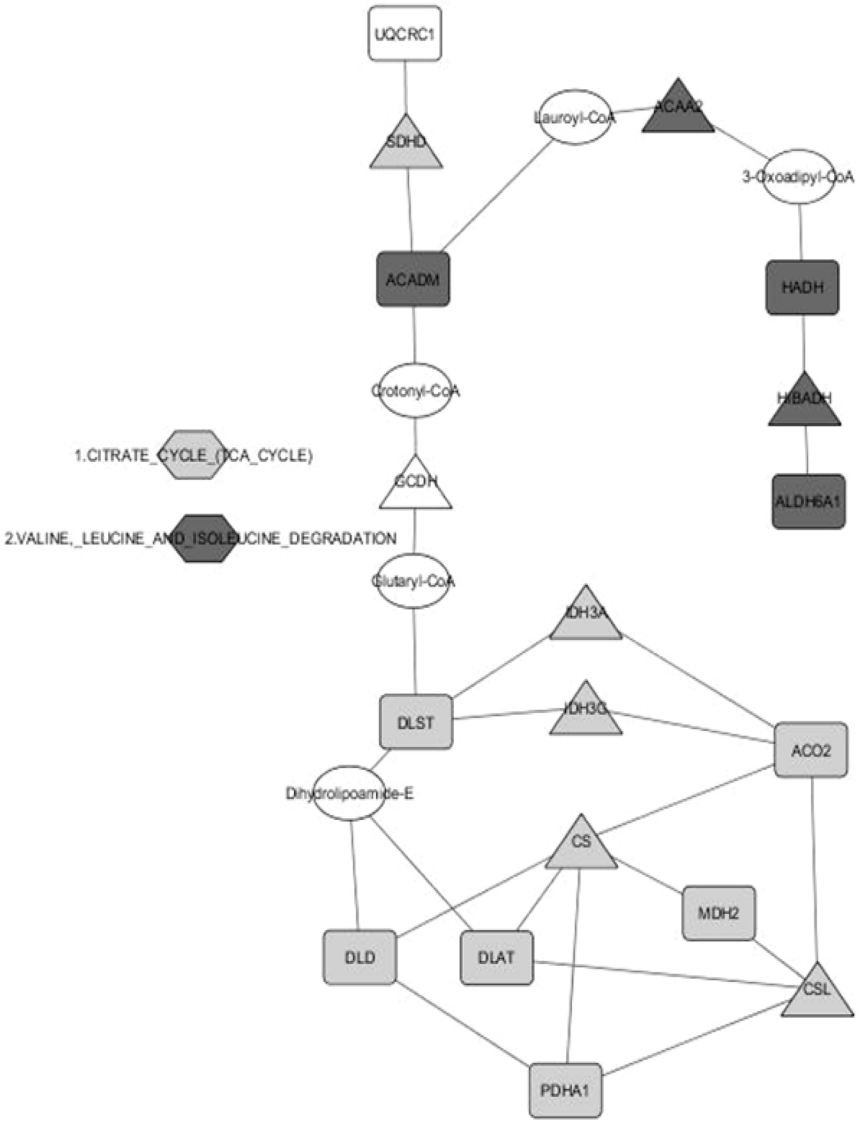

Figure 4. Enriched networks obtained by the Bioprofiling (http://www.bioprofiling.de/) online tool. Results obtained by R spider analysis after the submission of the input list containing carbonylated proteins found in this study. A maximum of one intermediate node was allowed to be added. Network visualization was obtained using Cytoscape (http://www.cytoscape.org/). Input proteins are shown as rectangles, whereas enriched nodes are represented by triangles. Circles represent substrates or products for both connected genes. P-value < 0.01. See text for details. SDHD, succinate dehydrogenase mitochondrial; ACCA2, 3-ketoacyl-CoA thiolase; HIBADH, 3-hydroxyisobutyrate dehydrogenase mitochondrial; GCDH, glutaryl-CoA dehydrogenase, mitochondrial; IDH, isocitrate dehydrogenase [NAD] subunit alpha, mitochondrial, IDH3G, isocitrate dehydrogenase [NAD] subunit gamma, mitochondrial; CS, citrate synthase; CSL, citrate synthase like; abbreviations for input proteins are reported in Table 1.

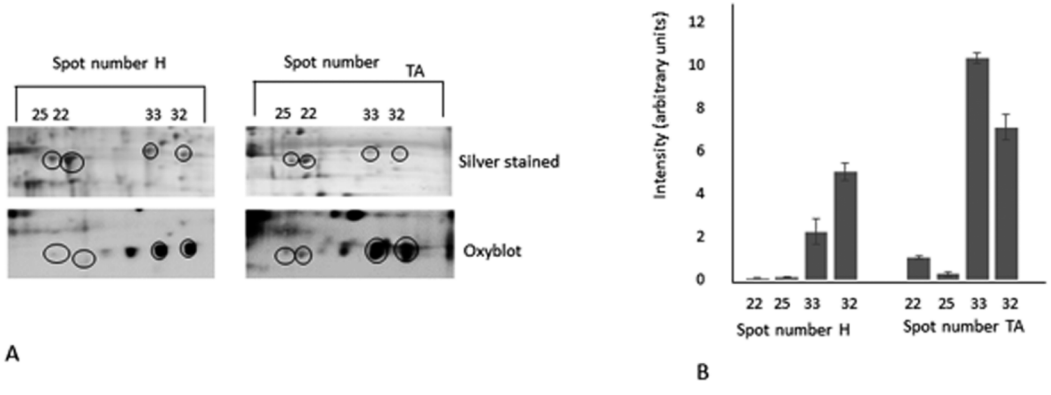

Figure 5. Carbonylation level does not correlate with the protein abundance. The intensity of spots 32, 33, 22, and 25 was evaluated in Oxyblot and silver stained gel (A). Histogram (B) represents the ratio between %Vspot in Oxyblot and %Vspot in silver stained gel.

DOI: 10.1021/acs.jproteome.6b00475
J. Proteome Res. 2016, 15, 3666−3678

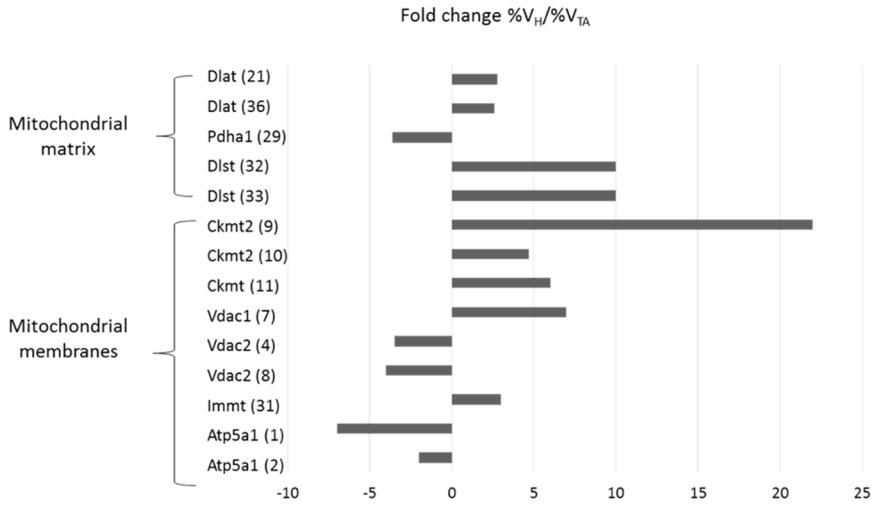

Figure 6. Histogram of differentially carbonylated proteins in H versus TA mitochondria in untrained mice. Bars represent the ratio between the average %V of the same spot in H and TA (H/TA). This %V is obtained by averaging the %V of the same spot from the five control animals. The differences between the mean values of H and TA are significant (p-value < 0.05) Proteins are indicated according to UniProtKB gene name (www.uniprot.org), and the number of corresponding spots is indicated.

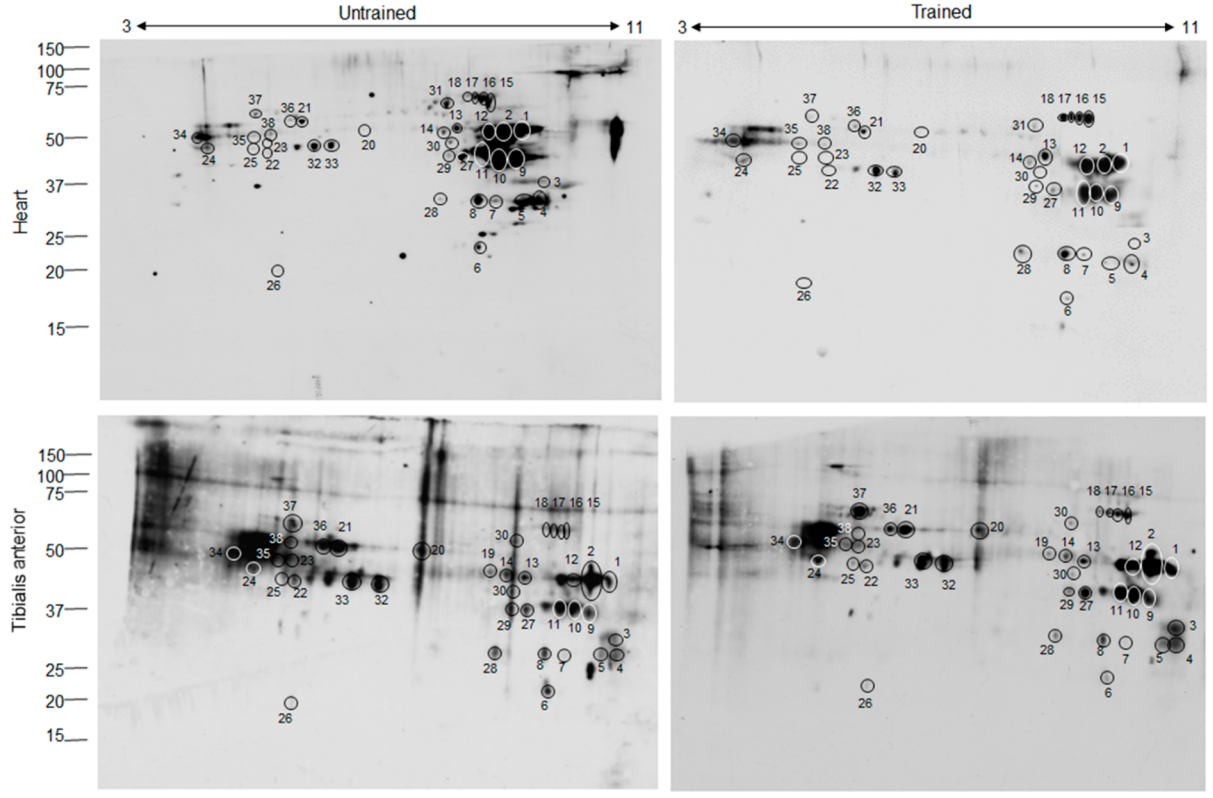

Figure 7. Oxyblots with anti-DNP antibodies to detect DNPH-reactive carbonyl groups in mitochondrial proteins. Proteins of H and TA from untrained and trained mice were separated by IEF, and carbonylated proteins were derivatized with DNPH in the strip (11 cm, 3−10 NL). Circles (black and white) indicated spots for which carbonylation was affected by training. Numbers indicate spots identified by MS.

carbonylation (Figure 5). Among this last group of spots, we found spots 32 and 33 (dihydrolipoyllysine-residue succinyltransferase component of 2-oxoglutarate dehydrogenase).

Furthermore, the difference in the intensity of carbonylation of the same spot between H and TA was investigated. The intensity of carbonylated spots on Oxyblots was normalized vs their respective spots visualized on silver stained gels. The bars represent the ratio between the average %V (normalized as specified above) of the same spot in H and TA (H/TA). The result was reported in Figure 6. Although it is not possible to draw a general conclusion, there is a trend of the proteins of the H to be more subjected to the carbonylation process.

Training-Induced Protein Carbonylation Modification

In order to investigate the effect of a regular aerobic (endurance) training protocol on mitochondria protein oxidation, five mice were regularly trained as specified in the Experimental Section. Mitochondrial proteins from trained and

DOI: 10.1021/acs.jproteome.6b00475
J. Proteome Res. 2016, 15, 3666−3678

Table 2. Identity of H and TA Mitochondrial Proteins Whose Carbonylation Level Was Affected by Training

Spot number	AC	Protein name	Fold change ($\%V_{trained}$ /$\%V_{untrained}$)
		Heart	
1	Q03265	ATP synthase subunit alpha, mitochondrial	−3
3	P08249	Malate dehydrogenase, mitochondrial	−3.8
4	Q60932	Voltage-dependent anion-selective channel protein 1 ATP synthase subunit alpha, mitochondrial	−4.6
5	Q60932	Voltage-dependent anion-selective channel protein 1	−3.3
6	Q9CZ13	Cytochrome *b*-c1 complex subunit 1, mitochondrial	−2.5
9	Q6P8J7	Creatine kinase S-type, mitochondrial	−6.5
10	P45952	Medium-chain specific acyl-CoA dehydrogenase, mitochondrial	−8.3
13	Q9EQ20	Methylmalonate-semialdehyde dehydrogenase [acylating], mitochondrial	2.1
17	Q99KI0	Aconitate hydratase, mitochondrial	1.8
		Tibialis Anterior	
1	Q03265	ATP synthase subunit alpha, mitochondrial	8
2	Q03265	ATP synthase subunit alpha, mitochondrial	4.5
3	P08249	Malate dehydrogenase, mitochondrial	2
9	Q6P8J7	Creatine kinase S-type, mitochondrial	2.9
15	Q99KI0	Aconitate hydratase, mitochondrial	2.4
16	Q99KI0	Aconitate hydratase, mitochondrial	2
27	P35486	Pyruvate dehydrogenase E1 component sub unit alpha, somatic form, mitochondrial	2.3

untrained mice were separated on 11 cm nonlinear IPG strips, and the strips were derivatized with DNPH followed by SDS-PAGE and Oxyblot. The intensity of carbonylated spots on Oxyblots was normalized vs their respective spots visualized on silver stained gels, and only the reproducible differences were taken into account (Figure 2S shows both silver-stained gels used for normalization and Coomassie-stained PVDF membrane used to check the transfer efficiency). Figure 7 shows a representative image of H and TA mitochondrial protein Oxyblots obtained from untrained and trained animals. The data are presented in Table 2, where, for each spot, the fold change (%Vtrained/ %Vuntrained, with $p \leq 0.05$) was reported. Interestingly, training affected differently the protein carbonylation of H and TA mitochondria. In fact, in TA, we found 7 spots corresponding to 5 different proteins whose carbonylation increases ($p \leq 0.05$). Among these proteins, we found two membrane proteins (ATP synthase subunit alpha, mitochondrial, and creatine kinase S-type) and three matrix proteins (aconitate hydratase, pyruvate dehydrogenase E1 component subunit alpha, and malate dehydrogenase). Differently in H mitochondria, we found 5 proteins (creatin kinase S type, malate dehydrogenase, medium-chain specific acyl-CoA dehydrogenase, ATP synthase alpha proteins, and voltage-dependent anion-selective channel protein 1) whose level of oxidation decreases and only two (aconitate hydratase and methylmalonate-semialdehyde dehydrogenase) that show an increased oxidation level.

Identification of Sites of Oxidative Modifications

LC-MS/MS analysis was employed to find oxidative modification in the identified proteins. It is well-known, in fact, that oxidative stress leads to a mixture of protein modifications, including carbonylation. Oxidation of the side-chains of lysine, arginine, and proline to aldehyde groups (as well as threonine to a ketone) are common modifications. However, histidine oxidation and tyrosine nitration are other oxidative modifications, and oxidizing conditions are expected to generate hydroxylation, chlorination, and oxygen addition (i.e., methionine or histidine oxide formation) at the level of specific amino acids.[38]

Within the different proteins, several peptides were found to be modified. Along with protein name, Table 1S reports modified peptides and the kind of the modification occurring within the peptide sequence. As for PTMs, this analysis led us to identify more than 40 oxidation sites within identified proteins. In particular, we detected 242 modified peptides, 73.1% resulted from the TA sample, while 26.8% from cardiac tissue. Among the identified sites, the oxidation of methionine to methionine sulfoxide appeared more frequently than the other oxidative modifications, although we cannot exclude the possibility that methionine oxidation might be related to protein extraction too. Moreover, some nitration sites were also detected. Among the proteins with nitrated tyrosines, we found ATP synthase subunit alpha and aconitate hydratase in TA and creatin kinase S type in H. Among typical carbonylation modifications, we found pyr-Glu, ketobutyric acid, and Pro-GluSA. Some of these modifications are located in important domains of mitochondrial proteins. For instance, Pyr-Glu modification found in ATP synthase alpha in H is located in positions 212−219, corresponding to the conserved region of the nucleotide binding domain of the enzyme.[39]

Creatin kinase S type, ATP synthase alpha, aconitate hydratase, and malate dehydrogenase are the proteins in which a major number of oxidative modifications were found. In Figure 3S of the Supporting Information, the modifications are indicated on the primary and tertiary structures of the enzyme aconitase.

Figure 8 displays several representative MS/MS fragmentation spectra on aconitate hydratase and ATP synthase.

DISCUSSION AND CONCLUSION

Several studies have detected changes in the total amount of carbonyl after different kinds of exercises, although few identified the specific targets of this oxidation. Since mitochondria play a key role in energy production and ROS formation, in this study we focused our attention on mitochondria protein carbonylation both under basal conditions (untrained mice) and after moderate training. The basal level of carbonylation seems to involve the same proteins in TA and H: in fact, the global pattern of carbonylation does not

DOI: 10.1021/acs.jproteome.6b00475
J. Proteome Res. 2016, 15, 3666−3678

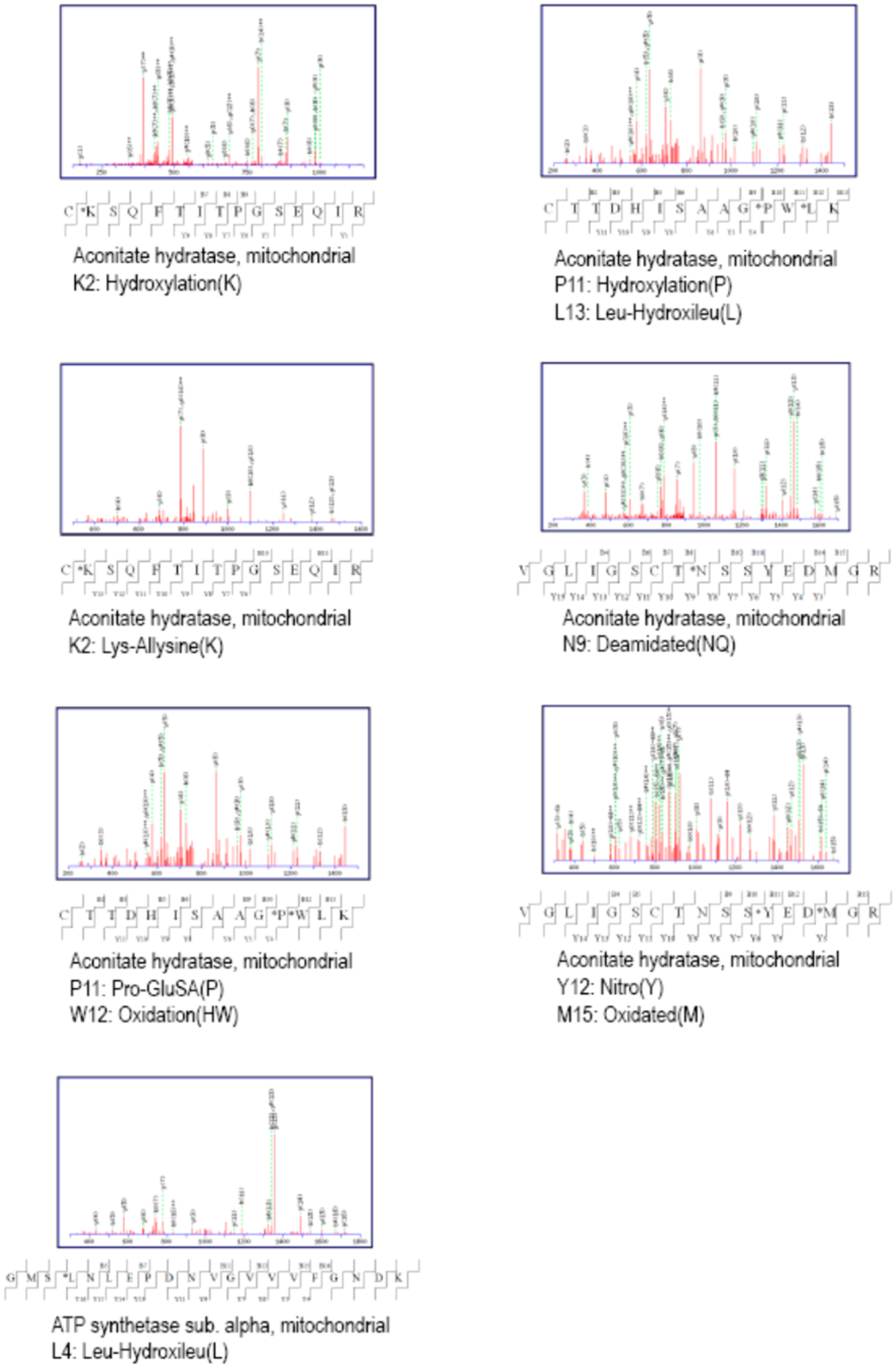

Figure 8. MS/MS fragmentation spectra showing the occurrence of oxidation (Leu-HydroxiLeu) on ATP synthase and several different oxidation sites on aconitate hydratase. For the MS/MS scans, the resolution was set to 15,000 and 10 ppm as peptide mass tolerance was applied.

present differences. Several proteins (Ckme2, Atp5a1, Dlat, Dlst, Vdac1, Atp5a1, and Atp5b) were found carbonylated in previous studies.[22,40,41] Some proteins in H resulted more carbonylated than in skeletal muscle, in particular Vdac1, Vdac2, Ckme2, and Atp5a1 that are situates in mitochondria membrane. Interestingly, the impact of training on H and TA protein oxidation appears different: in fact, in H mitochondria we observe a decrease of carbonylation level (with the exception of aconitate hydratase and ATP synthase subunit alpha) while in TA the general trend is represented by an increase of oxidation. This increase is consistent with that observed in other studies where a different animal model was used.[22,23] One possible explanation of this difference can be based on the fact that H and TA mitochondria are involved in

DOI: 10.1021/acs.jproteome.6b00475
J. Proteome Res. 2016, 15, 3666−3678

different types of nutrient metabolisms although both muscles require a constant supply of energy to support contractile activity. In fact, in the heart this obligation is met by the daily synthesis of ATP via oxidative phosphorylation, mostly by the catabolism of free fatty acids via β-oxidation and in tibialis anterior, which is a predominantly fast contracting muscle, by glycolysis and fermentation. Furthermore, the antioxidant systems also seem to differ between heart and skeletal muscle mitochondria. In fact, both have, as major antioxidant enzymes, manganese superoxide dismutase (MnSOD) and glutathione peroxidase (GPx), but interestingly, catalase (CAT) results present only in heart mitochondria and not in skeletal ones (MitoCarta2.0).[42−44] These characteristics could be involved in the differences observed in this study. In fact, we can speculate that, under basal conditions, the oxidative metabolism in H could produce a higher oxidation level of mitochondrial proteins than in TA, where glycolysis and fermentation are prevalently used to obtain energy. On the other hand, the increased protein carbonylation level observed in TA after exercise could reflect the inability of fermentative skeletal muscle to cope with the exercise-induced ROS production. In fact, endurance training is known to activate mitochondrial biogenesis and oxidative metabolism and, furthermore, in white muscle, a switch from fast twitch fibers to slow twitch fibers, that is combined with an increased aerobic metabolism.[45,46] This could be associated with an increase of ROS production during exercise. In fact, several studies demonstrate that contracting skeletal muscle is an important source for the generation of free radicals during exercise (recently reviewed by Jackson et al.).[47] This increase could be responsible for the increase of several oxidative markers observed after exercise. It must be underlined that this condition could be transient, since it has been demonstrated that the exercise-induced oxidative environment upregulates antioxidant enzymes and molecular chaperones[48] and that ROS production is essential for muscle adaptation.[45]

In this study, we also identified the specific oxidation sites of proteins that resulted carbonylated in oxyblot experiments. It was reported that MCO is one of the most important causes of protein carbonylation in living cells.[49] MCO occurs when reduced metal ions, such as Fe^{2+}, Cu^{+}, and Mn^{2+} interact with H_2O_2 in the Fenton reaction, producing the extremely reactive hydroxyl radicals, that directly oxidize amino acids in protein chains or cause protein backbone cleavage. It is believed that the metal catalyzed oxidation of proteins is a site-specific process, as the MCO carbonyl sites are limited to Arg, Lys, Pro, and Thr residues. MCO seems to occur preferentially when a metal ion is present in the protein structure and/or when proteins are located in proximity of ROS-generating sites. Furthermore, carbonylation sites have a strong tendency to occur in close proximity to each other, and for reasons yet uncertain, carbonylation seems to occur less in the N-terminal part of the proteins.[38,50] Proteins identified as strongly oxidized in this study present several characteristics which are typical of proteins subjected to carbonylation: clearly, the proteins are located in mitochondria that are an important source of ROS generation; furthermore, several of them have a metal ion in the protein structure (aconitate hydratase, has an iron−sulfur cluster; cytochrome *b*-c1 subunit has a zinc binding site) and/or are localized in proximity of ROS generation sites, especially represented by complex I (that releases superoxide in the matrix) and complex III (that releases superoxide both in the matrix and in the intermembrane space).[5] In fact, complex I was found associated with several mitochondrial dehydrogenases, including 2-oxoglutarate dehydrogenase complex and mitochondrial malate dehydrogenase (both found as carbonylated in this study).[51] Interestingly, two enzymes found strongly oxidized in this study (2-oxoglutarate dehydrogenase and pyruvate dehydrogenase complex) are themselves sites of ROS production. In particular, it has been demonstrated that Dld (dihydrolipoyl dehydrogenase), which is a component of both these enzymes, is able to produce ROS.[52] These three enzymes were found associated in the Reactome pathway-based network (Figure 3) through an intermediate node represented by a lipoamide molecule. However, it should be mentioned that the difficulty in purification of mitochondrial membrane complexes and in their resolution through classical 2-DE may have led to an underestimation of their carbonylation

In both TA and H, exercise induces an increase of aconitase carbonylation. This enzyme has an iron−sulfur cluster that is vulnerable to ROS attack, a structural characteristic that has led to its use as an indicator of superoxide production.[5] Oxidation of this protein occurs mostly at the C-terminal of the proteins, where the binding sites for the iron−sulfur cluster and for the substrate are located (Figure 3S). Furthermore, when its FeS center is oxidized by superoxide, Fe^{3+} is released and this unprotected, free iron ion can trigger a Fenton reaction causing damage to proteins in its proximity. Since the Krebs cycle appears organized in a metabolon in the matrix,[53] it is reasonable to find others Krebs cycle enzymes to be carbonylated under oxidative stress because of the proximity of aconitase. Indeed, we found carbonylated malate dehydrogenase and 2-oxoglutarate dehydrogenase.

The important finding that can be extrapolated by our and other studies is that, in heart and skeletal muscle, as already observed for plasma proteins, there is a basal level of carbonylation that probably represents a physiological condition and that can undergo variation induced by regular exercise. The important questions are how much this basal level can be perturbed without causing deleterious effects for the cells and if there are specific proteins whose function is severely affected by carbonylation. In fact, in some cases the oxidation of proteins, such as aconitase, was related to aging and disease,[54] but how widespread the oxidative process should be to be dangerous for cellular function needs further investigation. The identification by the proteomic approach of the specific sites of oxidation can greatly contribute to answering these questions and to verifying if there is a cause−effect link between oxidation of specific proteins and the impairment of a specific cellular function.

■ ASSOCIATED CONTENT

Supporting Information

The Supporting Information is available free of charge on the ACS Publications website at DOI: 10.1021/acs.jproteome.6b00475.

Table 1S. Identification of sites of oxidative modifications. Figure 1S. Coomassie stained gels: (A) Tibialis anterior, (B) Heart. Circles and numbers indicate the identified spots. Figure 2S. Coomassie stained PVDF membrane (A) used to check the efficiency and the reproducibility of the blotting procedure and silver-stained gel (B) used to perform normalization. Figure 3S. Oxidized amino acids were indicated on the primary (a)

DOI: 10.1021/acs.jproteome.6b00475
J. Proteome Res. 2016, 15, 3666−3678

and tertiary (B) structure of mouse aconitate hydratase. (PDF)

AUTHOR INFORMATION

Corresponding Author

*E-mail: francesca.magherini@unifi.it.

Author Contributions

[¤]A.C. and T.G. contributed equally to this work

Notes

The authors declare no competing financial interest.

ACKNOWLEDGMENTS

This work was funded by a grant from Italian Ministry of University and Research (MIUR) (ALESSANDRAMODESTIRICATEN14).

ABBREVIATIONS USED

H, heart
TA, tibialis anterior
MS/MS, tandem mass spectrometry
2-DE, two-dimensional gel electrophoresis
Pyro-Glu, pyroglutamate
GluSA, glutamic semialdehyde
TCA, tricarboxylic acid cycle
MCO, metal catalyzed oxidation

REFERENCES

(1) Egan, B.; Zierath, J. R. Exercise Metabolism and the Molecular Regulation of Skeletal Muscle Adaptation. *Cell Metab.* **2013**, *17*, 162−184.

(2) Powers, S. K.; Jackson, M. J. Exercise-induced oxidative stress: cellular mechanisms and impact on muscle force production. *Physiol. Rev.* **2008**, *88*, 1243−1276.

(3) Sakellariou, G. K.; Vasilaki, A.; Palomero, J.; Kayani, A.; Zibrik, L.; McArdle, A.; Jackson, M. J. Studies of mitochondrial and non-mitochondrial sources implicate nicotinamide adenine dinucleotide phosphate oxidase(s) in the increased skeletal muscle superoxide generation that occurs during contractile activity. *Antioxid. Redox Signaling* **2013**, *2018*, 603−21.

(4) Pearson, T.; Kabayo, T.; Ng, R.; Chamberlain, J.; McArdle, A.; Jackson, M. J. Skeletal muscle contractions induce acute changes in cytosolic superoxide, but slower responses in mitochondrial superoxide and cellular hydrogen peroxide. *PLoS One* **2014**, *9*, e96378.

(5) Brand, M. D. The sites and topology of mitochondrial superoxide production. *Exp. Gerontol.* **2010**, *45*, 466−472.

(6) Muller, F. L.; Liu, Y.; Van Remmen, H. Complex III releases superoxide to both sides of the inner mitochondrial membrane. *J. Biol. Chem.* **2004**, *279*, 49064−49073.

(7) Sahlin, K.; Shabalina, I. G.; Mattsson, C. M.; Bakkman, L.; Fernström, M.; Rozhdestvenskaya, Z.; Enqvist, J. K.; Nedergaard, J.; Ekblom, B.; Tonkonogi, M. Ultraendurance exercise increases the production of reactive oxygen species in isolated mitochondria from human skeletal muscle. *J. Appl. Physiol.* **2010**, *108*, 780−787.

(8) Perevoshchikova, I. V.; Quinlan, C. L.; Orr, A. L.; Gerencser, A. A.; Brand, M. D. Sites of superoxide and hydrogen peroxide production during fatty acid oxidation in rat skeletal muscle mitochondria. *Free Radical Biol. Med.* **2013**, *61*, 298−309.

(9) Goncalves, R. L.; Quinlan, C. L.; Perevoshchikova, I. V.; Hey-Mogensen, M.; Brand, M. D. Sites of superoxide and hydrogen peroxide production by muscle mitochondria assessed ex vivo under conditions mimicking rest and exercise. *J. Biol. Chem.* **2015**, *290*, 209−227.

(10) St-Pierre, J.; Buckingham, J. A.; Roebuck, S. J.; Brand, M. D. Topology of superoxide production from different sites in the mitochondrial electron transport chain. *J. Biol. Chem.* **2002**, *277*, 44784−44790.

(11) Boveris, A.; Chance, B. The Mitochondrial Generation of Hydrogen Peroxide. *Biochem. J.* **1973**, *134*, 707−716.

(12) Barreiro, E.; Hussain, S. N. Protein carbonylation in skeletal muscles: impact on function. *Antioxid. Redox Signaling* **2010**, *12*, 417−429.

(13) Dalle-Donne, I.; Rossi, R.; Giustarini, D.; Milzani, A.; Colombo, R. Protein carbonyl groups as biomarkers of oxidative stress. *Clin. Chim. Acta* **2003**, *329*, 23−38.

(14) Bloomer, R. J.; Fry, A. C.; Falvo, M. J.; Moore, C. A. Protein carbonyls are acutely elevated following single set anaerobic exercise in resistance trained men. *J. Sci. Med. Sport.* **2007**, *10*, 411−417.

(15) Bloomer, R. J.; Goldfarb, A. H.; Wideman, L.; McKenzie, M. J.; Consitt, L. A. Effects of Acute Aerobic and Anaerobic Exercise on Blood Markers of Oxidative Stress. *J. Strength Cond. Res.* **2005**, *19*, 276.

(16) Falone, S.; Mirabilio, A.; Pennelli, A.; Cacchio, M.; Di Baldassarre, A.; Gallina, S.; Passerini, A.; Amicarelli, F. Differential impact of acute bout of exercise on redox-and oxidative damage-related profiles between untrained subjects and amateur runners. *Physiol. Res.* **2010**, *59*, 953−961.

(17) Lamprecht, M.; Greilberger, J. F.; Schwaberger, G.; Hofmann, P.; Oettl, K. Single bouts of exercise affect albumin redox state and carbonyl groups on plasma protein of trained men in a workload-dependent manner. *J. Appl. Physiol.* **2008**, *104*, 1611−1617.

(18) Bayod, S.; del Valle, J.; Lalanza, J. F.; Sanchez-Roige, S.; de Luxán-Delgado, B.; Coto-Montes, A.; Canudas, A. M.; Camins, A.; Escorihuela, R. M.; Pallàs, M. Long-term physical exercise induces changes in sirtuin 1 pathway and oxidative parameters in adult rat tissues. *Exp. Gerontol.* **2012**, *47*, 925−935.

(19) Radák, Z.; Ogonovszky, H.; Dubecz, J.; Pavlik, G.; Sasvari, M.; Pucsok, J.; Berkes, I.; Csont, T.; Ferdinandy, P. Super-marathon race increases serum and urinary nitrotyrosine and carbonyl levels. *Eur. J. Clin. Invest.* **2003**, *33*, 726−730.

(20) Ramos, D.; Martins, E. G.; Viana-Gomes, D.; Casimiro-Lopes, G.; Salerno, V. P. Biomarkers of oxidative stress and tissue damage released by muscle and liver after a single bout of swimming exercise. *Appl. Physiol., Nutr., Metab.* **2013**, *38*, 507−11.

(21) Silva, L. A.; Pinho, C. A.; Scarabelot, K. S.; Fraga, D. B.; Volpato, A. M. J.; Boeck, C. R.; Souza, C. T.; Streck, E. L.; Pinho, R. A. Physical exercise increases mitochondrial function and reduces oxidative damage in skeletal muscle. *Eur. J. Appl. Physiol.* **2009**, *105*, 861−867.

(22) Magherini, F.; Abruzzo, P. M.; Puglia, M.; Bini, L.; Gamberi, T.; Esposito, F.; Veicsteinas, A.; Marini, M.; Fiorillo, C.; Gulisano, M.; Modesti, A. Proteomic analysis and protein carbonylation profile in trained and untrained rat muscles. *J. Proteomics* **2012**, *75*, 978−992.

(23) Magherini, F.; Gamberi, T.; Pietrovito, L.; Fiaschi, T.; Bini, L.; Esposito, F.; Marini, M.; Abruzzo, P. M.; Gulisano, M.; Modesti, A. Proteomic and Carbonylation Profile Analysis of Rat Skeletal Muscles following Acute Swimming Exercise. *PLoS One* **2013**, *8*, e71839.

(24) Guidi, F.; Magherini, F.; Gamberi, T.; Bini, L.; Puglia, M.; Marzocchini, R.; Ranaldi, F.; Modesti, P. A.; Gulisano, M.; Modesti, A. Plasma protein carbonylation and physical exercise. *Mol. BioSyst.* **2011**, *7*, 640−650.

(25) Hamada, T.; Arias, E. B.; Cartee, G. D. Increased submaximal insulin-stimulated glucose uptake in mouse skeletal muscle after treadmill exercise. *J. Appl. Physiol.* **2006**, *101*, 1368−1376.

(26) Kemi, O. J.; Loennechen, J. P.; Wisløff, U.; Ellingsen, Ø. Intensity-controlled treadmill running in mice: cardiac and skeletal muscle hypertrophy. *J. Appl. Physiol.* **2002**, *93*, 1301−1309.

(27) Fernando, P.; Bonen, A.; Hoffman-Goetz, L. Predicting submaximal oxygen consumption during treadmill running in mice. *Can. J. Physiol. Pharmacol.* **1993**, *71*, 854−7.

(28) Nocella, M.; Cecchi, G.; Bagni, M. A.; Colombini, B. Force enhancement after stretch in mammalian muscle fiber: no evidence of cross-bridge involvement. *AJP Cell Physiol.* **2014**, *307*, C1123−C1129.

(29) Frezza, C.; Cipolat, S.; Scorrano, L. Organelle isolation: functional mitochondria from mouse liver, muscle and cultured fibroblasts. *Nat. Protoc.* **2007**, *2*, 287−95.

DOI: 10.1021/acs.jproteome.6b00475
J. Proteome Res. 2016, 15, 3666−3678

(30) Hochstrasser, D. F.; Patchornik, A.; Merril, C. R. Development of polyacrylamide gels that improve the separation of proteins and their detection by silver staining. *Anal. Biochem.* **1988**, *173*, 412−423.
(31) Neuhoff, V.; Arold, N.; Taube, D.; Ehrhardt, W. Improved staining of proteins in polyacrylamide gels including isoelectric focusing gels with clear background at nanogram sensitivity using Coomassie Brilliant Blue G-250 and R-250. *Electrophoresis* **1988**, *9*, 255−262.
(32) Zhang, B.; Kirov, S.; Snoddy, J. WebGestalt: An integrated system for exploring gene sets in various biological contexts. *Nucleic Acids Res.* **2005**, *33*, 741−748.
(33) Antonov, A. V.; Schmidt, E. E.; Dietmann, S.; Krestyaninova, M.; Hermjakob, H. R spider: a network-based analysis of gene lists by combining signaling and metabolic pathways from Reactome and KEGG databases. *Nucleic Acids Res.* **2010**, *38*, W78−W83.
(34) Antonov, A. V. BioProfiling.de: Analytical web portal for high-throughput cell biology. *Nucleic Acids Res.* **2011**, *39*, 323−327.
(35) Shannon, P.; Markiel, A.; Ozier, O.; Baliga, N. S.; Wang, J. T.; Ramage, D.; Amin, N.; Schwikowski, B.; Ideker, T. Cytoscape \rCytoscape: a software environment for integrated models of biomolecular interaction networks. *Genome Res.* **2003**, *13*, 2498−2504.
(36) Giorgi, C.; Missiroli, S.; Patergnani, S.; Duszynski, J.; Wieckowski, M. R.; Pinton, P. Mitochondria-Associated Membranes: Composition, Molecular Mechanisms, and Physiopathological Implications. *Antioxid. Redox Signaling* **2015**, *22*, 995−1019.
(37) Anesti, V.; Scorrano, L. The relationship between mitochondrial shape and function and the cytoskeleton. *Biochim. Biophys. Acta, Bioenerg.* **2006**, *1757*, 692−699.
(38) Temple, A.; Yen, T. Y.; Gronert, S. Identification of Specific Protein Carbonylation Sites in Model Oxidations of Human Serum Albumin. *J. Am. Soc. Mass Spectrom.* **2006**, *17*, 1172−1180.
(39) Boyer, P. D. The ATP synthase–a splendid molecular machine. *Annu. Rev. Biochem.* **1997**, *66*, 717−49.
(40) Fedorova, M.; Kuleva, N.; Hoffmann, R. Identification, quantification, and functional aspects of skeletal muscle protein-carbonylation in vivo during acute oxidative stress. *J. Proteome Res.* **2010**, *9*, 2516−2526.
(41) Marin-Corral, J.; Fontes, C. C.; Pascual-Guardia, S.; Sanchez, F.; Olivan, M.; Argilés, J. M.; Busquets, S.; López-Soriano, F. J.; Barreiro, E. Redox balance and carbonylated proteins in limb and heart muscles of cachectic rats. *Antioxid. Redox Signaling* **2010**, *12*, 365−380.
(42) Calvo, S. E.; Clauser, K. R.; Mootha, V. K. MitoCarta2.0: an updated inventory of mammalian mitochondrial proteins. *Nucleic Acids Res.* **2016**, *44*, 1251−7.
(43) Phung, C. D.; Ezieme, J. A.; Turrens, J. F. Hydrogen peroxide metabolism in skeletal muscle mitochondria. *Arch. Biochem. Biophys.* **1994**, *315*, 479−82.
(44) Radi, R.; Turrens, J. F.; Chang, L. Y.; Bush, K. M.; Crapo, J. D.; Freeman, B. A. Detection of catalase in rat heart mitochondria. *J. Biol. Chem.* **1991**, *266*, 22028−22034.
(45) Ferraro, E.; Giammarioli, A. M.; Chiandotto, S.; Spoletini, I.; Rosano, G. Exercise-Induced Skeletal Muscle Remodeling and Metabolic Adaptation: Redox Signaling and Role of Autophagy. *Antioxid. Redox Signaling* **2014**, *21*, 154−176.
(46) Bassel-Duby, R.; Olson, E. N. Signaling pathways in skeletal muscle remodeling. *Annu. Rev. Biochem.* **2006**, *75*, 19−37.
(47) Jackson, M. J.; Vasilaki, A.; McArdle, A. Cellular mechanisms underlying oxidative stress in human exercise. *Free Radical Biol. Med.* **2016**, *98*, 13−17.
(48) Gomez-Cabrera, M. C.; Domenech, E.; Viña, J. Moderate exercise is an antioxidant: Upregulation of antioxidant genes by training. *Free Radical Biol. Med.* **2008**, *44*, 126−131.
(49) Møller, I. M.; Rogowska-Wrzesinska, A.; Rao, R. S. P. Protein carbonylation and metal-catalyzed protein oxidation in a cellular perspective. *J. Proteomics* **2011**, *74*, 2228−2242.
(50) Maisonneuve, E.; Ducret, A.; Khoueiry, P.; Lignon, S.; Longhi, S.; Talla, E.; Dukan, S. Rules governing selective protein carbonylation. *PLoS One* **2009**, *4*, e7269.
(51) Sumegi, B.; Srere, P. A. Complex I binds several mitochondrial NAD-coupled dehydrogenases. *J. Biol. Chem.* **1984**, *259*, 15040−15045.
(52) Starkov, A. A.; Fiskum, G.; Chinopoulos, C.; Lorenzo, B. J.; Browne, S. E.; Patel, M. S.; Beal, M. F. Mitochondrial α-Ketoglutarate Dehydrogenase Complex Generates Reactive Oxygen Species. *J. Neurosci.* **2004**, *24*, 7779−7788.
(53) Robinson, J. B.; Srere, P. A. Organization of Krebs tricarboxylic acid cycle enzymes. *Biochem. Med.* **1985**, *33*, 149−57.
(54) Lushchak, O. V.; Piroddi, M.; Galli, F.; Lushchak, V. I. Aconitase post-translational modification as a key in linkage between Krebs cycle, iron homeostasis, redox signaling, and metabolism of reactive oxygen species. *Redox Rep.* **2014**, *19*, 8−15.

DOI: 10.1021/acs.jproteome.6b00475
J. Proteome Res. 2016, 15, 3666−3678